Thermodynamic and Kinetic Properties of the Formation of $Mn_2P_2O_7$ by Thermal Decomposition of $Mn(H_2PO_2)_2 \cdot H_2O$

Pittayagorn Noisong,[†] Chanaiporn Danvirutai,*[,†] and Banjong Boonchom[‡]

Department of Chemistry and Center of Excellence for Innovation in Chemistry (PERCH-CIC), Faculty of Science, Khon Kaen University, Khon Kaen 40002, Thailand, and King Mongkut's Institute of Technology Ladkrabang, Chumphon Campus, 17/1 M. 6 Pha Thiew District, Chumphon 86160, Thailand

The kinetic properties in terms of activation energies and pre-exponential factors of two decomposition stages of $Mn(H_2PO_2)_2 \cdot H_2O$ were calculated through the isoconversional method of Kissinger. The calculated results were further used to calculate some transition-state thermodynamic functions ($\Delta H^{\ddagger}$, $\Delta S^{\ddagger}$, $\Delta G^{\ddagger}$) of the transition-state complex according to the transition-state complex theory of Erying. Kinetic and thermodynamic results are consistent with the indication that the two steps are nonspontaneous before the introduction of heat is involved. The Avrami constant, n, of the two decomposition steps was calculated and interpreted to be responsible for the mechanism of 1D growth decomposition, which is a nucleation controlled mechanism. Vibrational frequencies of breaking bonds in two stages were estimated and assigned by comparison with the observed FTIR spectra. The results exhibit a very close correlation between calculated and observed values.

Introduction

Metal pyrophosphates are currently of considerable industrial interest because of their utility as catalysts ($(VO)_2P_2O_7$),[1] laser hosts ($NaPrP_2O_7$),[2] and magnetic materials ($Fe_2P_2O_7$).[3] The well-known series of pyrophosphate $M_2P_2O_7$ (M = Mn, Ni, Ag, Zn, Cr, Co, and Sn) are used as catalysts.[4,5] In addition, calcium pyrophosphate (CaP_2O_7) is an important compound in bone related processes.[6] A phosphorus compound that is closely related to this group is manganese hypophosphite because of its wide applications, as reported in our previous work.[7] It is mainly used in the pharmaceutical, polymer, and chemical intermediate manufacturing fields. The thermal decomposition of this compound has already been studied and reported in our previous paper.[7] The final decomposition product of $Mn(H_2PO_2)_2 \cdot H_2O$ is manganese pyrophosphate ($Mn_2P_2O_7$), which exhibited interesting magnetic[8,9] and catalytic properties.[5] In the literature, $Mn_2P_2O_7$ had been prepared by heating $NH_4MnPO_4 \cdot 6H_2O$ to high temperature (1350 K); however, it is a complicated and energy consuming synthesis.[10]

Kinetic and thermodynamic studies have become a crucial point in thermal analysis, of which the main purposes are to determine the mechanism of decomposition and the formation processes and to calculate kinetic and thermodynamic parameters. The calculation of thermodynamic parameters from kinetic parameters is challenging and provides interesting new information, as exhibited in this Article. These data play an important role in theoretical study for application development and industrial production of a compound as a basis of theoretical analysis. The thermal stability of a chemical intermediate in connection with the thermal processing of this compound is one of the major fields of interest.

* To whom correspondence should be addressed. Tel: +66-43-202222 ext. 12243. Fax: +66-43-202373. E-mail: chanai@kku.ac.th.
[†] Khon Kaen University.
[‡] King Mongkut's Institute of Technology Ladkrabang.

The aim of the present work was to study the thermodynamic and kinetic parameters of the formation of $Mn_2P_2O_7$ from the decomposition of manganese hypophosphite monohydrate, $Mn(H_2PO_2)_2 \cdot H_2O$, by using thermogravimetric/differential thermogravimetric/differential thermal analysis (TG/DTG/DTA), X-ray diffraction (XRD), and Fourier transform infrared spectroscopy (FTIR). The nonisothermal decomposition kinetic analysis of $Mn(H_2PO_2)_2 \cdot H_2O$ under a nitrogen atmosphere in two decomposition steps was carried out by using the isoconversional method of Kissinger.[11,12] In addition, the mechanism of these steps was suggested through an Avrami constant. The wavenumbers of the activated bonds in two activation steps were estimated and compared with the observed values in FTIR spectra. The results will be discussed in terms of the decomposition mechanism and thermodynamic and kinetic parameters. The calculated thermodynamic functions ($\Delta H^{\ddagger}$, $\Delta S^{\ddagger}$, $\Delta G^{\ddagger}$) of the activated complex, kinetic parameters (A, E), and mechanism of the two decomposition reactions of $Mn(H_2PO_2)_2 \cdot H_2O$ are reported for the first time.

Experimental Section

The manganese hypophosphite monohydrate precursor was synthesized[7,13] and characterized according to our previous work.[7] Thermal analysis measurements (TG/DTG/DTA) were carried out using a Pyris Diamond Perkin-Elmer apparatus with α-Al_2O_3 powder as the reference material. The experiments were performed at the heating rates of (10, 15, 20, and 25) $K \cdot min^{-1}$ over the temperature range from (303.15 to 723.15) K under a N_2 atmosphere at a flow rate of 100 $mL \cdot min^{-1}$. The sample mass of ca. (6.0 to 10.0) mg was placed in an aluminum crucible. The structure of the calcined products was studied by X-ray powder diffraction using an X-ray diffractometer (Phillips PW3040) with Cu Kα radiation (λ = 1.546 Å) and an FTIR/FT Raman spectrophotometer (Perkin-Elmer spectrum GX) with 16 scans in the range of (4000 to 370) cm^{-1} and a resolution of 4 cm^{-1}.

10.1021/je8006748 CCC: $40.75
Published on Web 02/20/2009

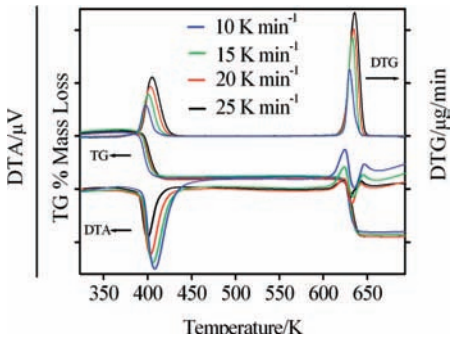

Figure 1. TG/DTG/DTA curves of the synthesized $Mn(H_2PO_2)_2 \cdot H_2O$ at four heating rates under a N_2 atmosphere.

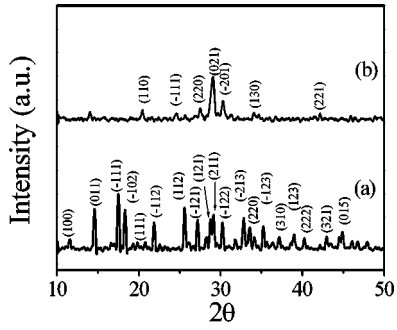

Figure 2. XRD patterns of (a) the synthesized $Mn(H_2PO_2)_2 \cdot H_2O$ and (b) the calcined $Mn(H_2PO_2)_2 \cdot H_2O$ at 723 K under a N_2 atmosphere.

Results and Discussion

Thermal Decomposition Study. The TG/DTG/DTA curves of $Mn(H_2PO_2)_2 \cdot H_2O$ at four heating rates are shown in Figure 1. The TG curve shows the weight losses in two stages between (303.15 and 723.15) K, which are related to the elimination of water molecules and the phase transformation. The two stages are dehydration and decomposition steps, which are observed in two areas: (393 to 453) K and (603 to 643) K, respectively. Two endothermic peaks on the DTA curves at a heating rate of 10 $K \cdot min^{-1}$ are observed at (398.95 and 629.15) K, which correspond to DTG peaks at (398.95 and 629.95) K, respectively.

The total weight loss is 17.13 %. The first step yields a weight loss of 8.36 %, which corresponds to the elimination of water, and the second step (8.77 %) corresponds to the elimination of water and phosphine. The theoretical weight losses in the first and second steps are 8.84 % and 23.30 %, respectively. The observed results agree well with those calculated only for the first step. The consequent release of hydrogen and oxygen gases at high temperature (631.15 K) leads to the suggestion of the reaction between H_2 and O_2 to become H_2O. Evidence of this is the strong exothermic effect on the DTA curves in the second step. Therefore, the experimental and theoretical values are different in this step.

The reactions may be proposed as[14,15]

$$Mn(H_2PO_2)_2 \cdot H_2O \rightarrow \alpha\text{-}Mn(H_2PO_2)_2 \cdot xH_2O + yH_2O \quad (1)$$

$$\alpha\text{-}Mn(H_2PO_2)_2 \cdot xH_2O \rightarrow \frac{1}{2}Mn_2P_2O_7 + \left(\frac{1}{2} + x\right)H_2O + PH_3 \quad (2)$$

where $x + y = 1$.

The complete decomposition product of synthesized $Mn(H_2PO_2)_2 \cdot H_2O$ under a N_2 atmosphere was found to be $Mn_2P_2O_7$. This compound was confirmed by XRD (Figure 2) and FTIR data (Figure 3). The XRD patterns of the prepared $Mn(H_2PO_2)_2 \cdot H_2O$ and its final decomposition product

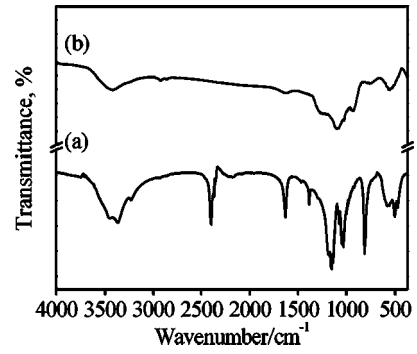

Figure 3. FT-IR spectra of (a) the synthesized $Mn(H_2PO_2)_2 \cdot H_2O$ and (b) the calcined $Mn(H_2PO_2)_2 \cdot H_2O$ at 433 K under a N_2 atmosphere.

($Mn_2P_2O_7$) are shown in Figure 2. All detectable peaks are indexed as synthesized $Mn(H_2PO_2)_2 \cdot H_2O$ and $Mn_2P_2O_7$ structures, which are identified using the standard data of PDF nos. 810649 and 771243, respectively. The FTIR spectra of manganese hypophosphite monohydrate and $Mn_2P_2O_7$ are presented in Figure 3. Three bands in the range of (3457 to 3231) cm^{-1} illustrated in Figure 3a are assigned to the O−H stretching modes, whereas the bands at (1632 and 1384) cm^{-1} are assigned to the bending mode of vibration of water molecules. Another three bands in the region of (2450 to 2300) cm^{-1} are attributed to the stretching mode of PH_2 and of phosphine (Figure 3a). The FTIR spectrum of the calcined $Mn(H_2PO_2)_2 \cdot H_2O$ at 723 K under a N_2 atmosphere (Figure 3b) illustrates the same characteristics as those of $Mn_2P_2O_7$.[7] The P−O stretching modes of the $[P_2O_7]^{4-}$ anion are known to appear in the (1250 to 975) cm^{-1} region.[7,16] The specificity of nonisothermal decomposition is due to the vibrational energy accumulated from the thermal field on a certain bond, which behaves according to anharmonic oscillators theory. The relationship between the isokinetic parameter, T_i, and the wavenumber of the activated bond was modified from the equation developed by Vlase et al. as follows[17,18]

$$\omega_{calcd} = \frac{k_B}{hc}T_i = 0.695T_i \quad (3)$$

and

$$\omega_{sp} = q\omega_{calcd} \quad (4)$$

where k_B are h are the Boltzmann and Planck's constants, respectively, c is the light velocity, q is the number of quanta ($q \in N$), and ω_{sp} is the assigned spectroscopic wavenumber for the bond that is supposed to break. The breaking of a certain bond in a molecule has an anharmonic behavior, and thus specific activation is also possible because of more than one quanta. We suggested the average maximum peak temperature, T_p, in the DTA curve for the calculation using eq 3. The average T_p values for the two transformation steps are (402.95 and 631.15) K, respectively. The ω_{calcd} values of two steps can be calculated from eq 3 and are tabulated in Table 1. These data reveal that the breaking of the O−H bonds in crystal water molecules (water of crystallization) and in the P−H bond in the studied compound occurred in the first and second steps as the elimination of H_2O and PH_3, respectively. The results exhibit very good agreement between the calculated wavenumber from the isokinetic temperature and the corresponding wavenumber from FTIR spectra for the bonds suggested to be broken.

Kinetics Study. The kinetic analyses can be carried out by various methods such as Kissinger's method and[12] Flynn−Wall−Ozawa,[19,20] Coats−Redfern,[21] Van Krevelens et al.,[22] and

Table 1. Comparison of Kinetic and Spectroscopic Data

β step	maximum temperature from DTA (K)				E_a	average T_p	ω_{calcd}	q	$q\omega_{calcd}$	ω_{sp} obsd in FTIR spectra[7]
K·min^{-1}	10	15	20	25	kJ·mol^{-1}	K	cm^{-1}		cm^{-1}	cm^{-1}
1	398.95	401.55	404.65	406.65	149.60	402.95	280.05	12	3360	3457−3231 (O−H in water)
								6	1680	1632
								5	1400	1384
2	629.35	630.65	631.95	632.65	823.49	631.15	438.65	5	2193	2398−2357 (P−H in PH_2)
								3	1315	1291
								2	877	815

Criado et al.[23] methods. The use of isoconversional or model-free methods (Kissinger, Ozawa, and Kissinger−Akahira−Sunose (KAS)) has recently increased because of the ability of these methods to calculate activation energy values without modelistic assumptions. In addition, the Kissinger method can be applied to calculate the pre-exponential factor, whereas the Ozawa and KAS methods can be used only to calculate the E values. The temperature corresponding to the maximum reaction rate (T_p) in the Kissinger method can be applied for estimation of the wavenumber of the activated bond using eq 3. In our previous work, the kinetic decomposition of $Mn(H_2PO_2)_2 \cdot H_2O$ has been studied by using the Ozawa and KAS methods.[7]

In the kinetic study of this compound, the Kissinger[11,12] equation is based on the calculation of activation energy from a point of the maximal temperature, T_p, and is widely used and well described in the literature,[24] owing to the accuracy of the obtained results. Therefore, the activation energy (E) and pre-exponential factors (A) for kinetic analysis of dehydration and decomposition reactions were determined by this method.

This method is based on the calculation of activation energy, E, and pre-exponential, A, from the plot between $\ln(\beta/T_p^2)$ and $1000/T_p$, as given in eq 5 (Kissinger equation)

$$\ln\left(\frac{\beta}{T_p^2}\right) = \ln\left(\frac{AR}{E}\right) - \left(\frac{E}{RT_p}\right) \quad (5)$$

where A is the pre-exponential factor (min^{-1}), E is the activation energy (kJ·mol^{-1}), β is the heating rate (K·min^{-1}), R is the gas constant (8.314 J·mol^{-1}·K^{-1}), and T_p is the peak temperature of the DTA curve that corresponds to the maximum reaction rate. According to the above-mentioned equation, plots of $\ln(\beta/T_p^2)$ against $(1000/T_p)$ can be obtained by a linear regression using a least-squares method. The activation energies, E, and pre-exponential factor can be calculated from the slope and intercept of the straight lines, respectively. According to the Kissinger equation, two thermal decomposition steps of the studied compound are plotted and shown in Figure 4. The activation energy of dehydration (step 1) and decomposition (step 2) was found

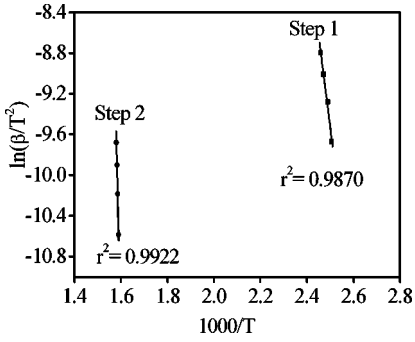

Figure 4. Kissinger plots for the dehydration (step 1) and decomposition (step 2) steps of $Mn(H_2PO_2)_2 \cdot H_2O$.

Table 2. Values of $\Delta S^{\ddagger}$, $\Delta H^{\ddagger}$, and $\Delta G^{\ddagger}$ for Dehydration and Decomposition Steps of $Mn(H_2PO_2)_2 \cdot H_2O$

parameter	dehydration step	decomposition step
$\Delta S^{\ddagger}$ (J·mol^{-1}·K^{-1})	120.52	1056.87
$\Delta H^{\ddagger}$ (kJ·mol^{-1})	146.22	818.22
$\Delta G^{\ddagger}$ (kJ·mol^{-1})	97.21	149.28

to be (149.61 ± 12.15) kJ·mol^{-1} ($r^2 = 0.9870$) and (823.46 ± 51.56) kJ·mol^{-1} ($r^2 = 0.9922$), respectively, whereas the pre-exponential factor of the two steps was found to be $4.55 \cdot 10^{19}$ min^{-1} and $5.78 \cdot 10^{68}$ min^{-1}, respectively. The activation energies were determined by the Ozawa and KAS methods in our previous publication[7] in which it was found that the first process is a single step, whereas the second step is a multistep process. However, the values of kinetic parameters (A and E) may not be the real values in the second step, which can be further studied.

A high activation energy value for the removal of all water molecules from manganese hypophosphite monohydrate is observed. The dehydration temperature at the intermediate temperature of 423.15 K was observed from TG/DTG/DTA experiments. The water molecules that were eliminated at the particular temperature can be classified as a crystal water type as well as coordinately linked water.[18,25] In the studied hydrate, it can be suggested that the water molecules are considered to be crystal water. These data indicated that the decomposition in the second step is harder than that in the first step, which demonstrates excellent agreement with the calculated wavenumber of the activated bond, ω_{calcd}. The similar results of the pre-exponential factor, which is used to measure the collision frequencies, reveal that the second step shows much higher collision frequencies compared with the first step. Therefore, decomposition in the second step should occur at an even higher-energy pathway. The thermal decomposition mechanism could be determined from the shape factor (n) of the endothermic peak represented by the following equation[26,27]

$$n = \frac{2.5}{\Delta T} \frac{T_0^2}{E_a/R} \quad (6)$$

where n is the Avrami constant, T_0 is the endothermic peak temperature, and ΔT is the full width at half-maximum (fwhm) of the endothermic peak at the highest heating rate. The n values of the two decomposition steps were found to be 1.14 and 1.44, respectively. Furthermore, this also implies that the second step should be interpreted to occur by a more complicated mechanism than that of the first step. Values of $n \approx 3$, 2, and 1 indicate 3D growth (spheres or hemispheres), 2D growth (disks and cylinders), and linear growth,[28] respectively. Therefore, the smaller n values in this study suggest that the dehydration and decomposition are dominated by a surface decomposition mechanism rather than by volume decomposition and that the

decomposition dimension is low[29] (1D growth), which indicates that it is a nucleation-controlled mechanism.

Estimation of the Thermodynamic Parameter. From the pre-exponential factor or Arrhenius constant, the thermodynamic parameters were calculated by using the activated complex theory (transition state) of Eyring.[30−32] The following general equation may be written[32]

$$A = \left(\frac{e\chi k_B T_0}{h}\right) \exp\left(\frac{\Delta S^{\ddagger}}{R}\right) \quad (7)$$

where e is the Neper number ($e = 2.7183$), χ is the transition factor, which is unity for a monomolecular reaction, k_B is the Boltzmann constant ($k_B = 1.3806 \cdot 10^{-23}$ J·K^{-1}), h is Planck's constant ($h = 6.6261 \cdot 10^{-34}$ J·s), T_0 is the peak temperature of the DTA curve (corresponding stage in the highest heating rate), R is the gas constant ($R = 8.314$ J·K^{-1}·mol^{-1}), and $\Delta S^{\ddagger}$ is the entropy of the transition-state complex, which may be calculated as follows

$$\Delta S^{\ddagger} = R \ln \frac{Ah}{e\chi K_B T_0} \quad (8)$$

The heat ($\Delta H^{\ddagger}$) and Gibbs energy ($\Delta G^{\ddagger}$) of the transition-state complexes were calculated using eqs 9 and 10, respectively

$$\Delta H^{\ddagger} = E - RT_0 \quad (9)$$

$$\Delta G^{\ddagger} = \Delta H^{\ddagger} - T_0 \Delta S^{\ddagger} \quad (10)$$

where E is the activation energy (E_a) of the Kissinger method and $\Delta H^{\ddagger}$and $\Delta G^{\ddagger}$ are the enthalpy and Gibbs energy of transition-state complexes, respectively. Thermodynamic parameters calculated from eqs 8, 9, and 10 are summarized in Table 2. The positive value of $\Delta S^{\ddagger}$ indicates that the transition state is highly disordered compared with the initial state. This $\Delta S^{\ddagger}$ value suggests an increase in the degrees of freedom of rotation and vibration when the system approaches the transition state of the "fast" stage[32,33] in two decomposition steps, and the second step exhibited greater randomness (larger number of randomness) than the first step. The positive values of $\Delta G^{\ddagger}$ at all studied steps are due to the fact that the decomposition process is not spontaneous. The endothermic peaks in the DTA data agree well with the positive sign of the activation enthalpy ($\Delta H^{\ddagger}$). Therefore, the positivity of $\Delta G^{\ddagger}$ is determined by a small activation entropy and a positively large activation enthalpy according to eq 10. The relationship of activation energy, E_a, and activation enthalpy, $\Delta H^{\ddagger}$, of the two decomposition steps show that the E_a value of the second decomposition step is higher than that of the first decomposition step, which also results in the same effect in the $\Delta H^{\ddagger}$ value and indicated that the second step needs a higher-energy pathway than the first step. That means that the rate of the second step is lower than that of the first step of the decomposition. Therefore, the second decomposition step occurs harder than the first decomposition step, which corresponds well with the kinetics and calculated wavenumbers of the activated bonds.

Conclusions

Manganese hypophosphite monohydrate precursor decomposes in two steps, and the final product is manganese pyrophosphate ($Mn_2P_2O_7$). Kinetic analysis from nonisothermal TG data applying a model-fitting method was studied, and the results provide the calculated kinetic parameters. A correlation between the isokinetic temperature and the wavenumber of the activated complex assigned to the breaking bond is possible. Therefore, the thermal sensitive part of a molecule can be analyzed by means of an adequate processing of the thermogravimetric data and in connection with the FTIR spectra. The mechanism of the two decomposition steps can be assumed through the Avrami constant, n, values which indicate that nucleation and 1D growth belongs to a nucleation-controlled mechanism. The activation entropy, $\Delta S^{\ddagger}$, enthalpy, $\Delta H^{\ddagger}$, and Gibbs energy, $\Delta G^{\ddagger}$, of transition in two decomposition steps in manganese hypophosphite monohydrate can be calculated for the first time. These values relate the activation energy, pre-exponential factor, and the mechanism of dehydration and decomposition of the title compound. However, the thermodynamic and kinetic parameters may not be the real values in the second step, which can be further studied. The results can be applied to the production of $Mn_2P_2O_7$, which plays a large role in industrial applications.

Acknowledgment

We thank the Department of Chemistry, Faculty of Science, Khon Kaen University for providing research facilities.

Supporting Information Available:

$Mn(H_2PO_2)_2 \cdot H_2O$ and $Mn_2P_2O_7$ standard data. This material is available free of charge via the Internet at http://pubs.acs.org.

Literature Cited

(1) Imai, H.; Kamiya, Y.; Okuhara, T. Selective Oxidation of *n*-Butane Over Nanosized Crystallites of $(VO)_2P_2O_7$ Synthesized by an Exfoliation−Reduction Process of $VOPO_4 \cdot 2H_2O$ in a Mixture of 2-Butanol and Ethanol. *J. Catal.* **2007**, *251*, 195.

(2) Baril, M.; Assaaoudi, H.; Kozinski, J. A.; Butler, I. S. A High-Pressure, Raman Spectroscopic Study of Bis(pyrophosphato)tetrazinc(II) and -tetramanganese(II) Decahydrate Salts. *Inorg. Chim. Acta* **2007**, *360*, 3155.

(3) Parada, C.; Perles, J.; Sáez-Puche, R.; Ruiz-Valero, C.; Snejko, N. Crystal Growth, Structure, and Magnetic Properties of a New Polymorph of $Fe_2P_2O_7$. *Chem. Mater.* **2003**, *15*, 3347.

(4) Takita, Y.; Sano, K.-I.; Kurosaki, K.; Kawata, N.; Nishiguchi, H.; Ito, M.; Ishihara, T. Oxidative Dehydrogenation of Iso-butane to Iso-butene I. Metal Phosphate Catalysts. *Appl. Catal.* **1998**, *A167*, 49.

(5) Takitaa, Y.; Sano, K.-I.; Muraya, T.; Nishiguchi, H.; Kawata, N.; Ito, M.; Akbay, T.; Ishihara, T. Oxidative Dehydrogenation of Iso-butane to Iso-butene II. Rare Earth Phosphate Catalysts. *Appl. Catal.* **1998**, *A170*, 23.

(6) Nicholas, B. D.; Smith, J. L.; Kellman, R. M. Calcium Pyrophosphate Deposition of the Temporomandibular Joint With Massive Bony Erosion. *J. Oral. Maxillofac. Surg.* **2007**, *65*, 2086.

(7) Noisong, P.; Danvirutai, C.; Srithanratana, T.; Boonchom, B. Synthesis, Characterization and Non-isothermal Decomposition Kinetics of Manganese Hypophosphite Monohydrate. *Solid State Sci.* **2008**, *10*, 1598.

(8) Assaaoudi, H.; Butler, I. S.; Kozinski, J. A. Crystal Structure, Vibrational Spectra, and Thermal Decomposition and Nitrogen Adsorption Behaviour of a New Tetramanganese(II) Dipyrophosphate Decahydrate, $Mn_4(P_2O_7)_2 \cdot 10H_2O$. *J. Chem. Crystallogr.* **2006**, *36*, 723.

(9) Fowlis, D. C.; Stager, C. V. Antiferromagnetic Resonance in $Mn_2P_2O_7$. *Can. J. Phys.* **1972**, *50*, 2681.

(10) Stefanidis, T.; Nord, A. G. Structure Studies of Thortveitite-Like Dimanganese Diphosphate, $Mn_2P_2O_7$. *Acta Crystallogr.* **1984**, *C40*, 1995.

(11) Wang, Z.; Wang, J.; Dang, L. Thermal, Phase Transition and Spectral Studies in Erythromycin Pseudopolymorphs: Dihydrate and Acetone Solvate. *Cryst. Res. Technol.* **2006**, *12*, 1219.

(12) Kissinger, H. E. Reaction Kinetics in Differential Thermal Analysis. *Anal. Chem.* **1957**, *29*, 1702.

(13) Marcos, M. D.; Amoros, P.; Sapiña, F.; Beltrán, D. Crystal Structure and Magnetic Properties of α-$Mn(H_2PO_2) \cdot H_2O$. *J. Alloys. Compd.* **1992**, *188*, 133.

(14) Yagodin, A. Thermal Decomposition of Dihypophosphito-(urea)-copper(II). *J. Therm. Anal.* **1988**, *33*, 537.

(15) Wang, W.; Gao, X.; Zheng, L.; Lan, Y. Reductive Dechlorination of Polychlorinated Dibenzo-*p*-Dioxins and Dibenzofurans in MSWI Fly Ash by Sodium Hypophosphite. *Sep. Purif. Technol.* **2006**, *52*, 186.

(16) Assaaoudi, H.; Butler, I. S.; Kozinski, J.; Gariépy, F. B. Crystal Structure, Vibrational Spectra and Thermal Decomposition of a New Tetrazinc(II) Dipyrophosphate Decahydrate, $Zn_4(P_2O_7)_2 \cdot 10H_2O$. *J. Chem. Crystallogr.* **2005**, *35*, 49.
(17) Vlase, T.; Vlase, G.; Doca, M.; Doca, N. Specificity of Decomposition of Solids in Non-isothermal Conditions. *J. Therm. Anal. Calorim.* **2003**, *72*, 597.
(18) Boonchom, B.; Danvirutai, D. Thermal Decomposition Kinetics of $FePO_4 \cdot 3H_2O$ Precursor to Synthesize Spherical Nanoparticles $FePO_4$. *Ind. Eng. Chem. Res.* **2007**, *46*, 9071.
(19) Ozawa, T. A New Method of Analyzing Thermogravimetric Data. *Bull. Chem. Soc. Jpn.* **1965**, *38*, 1881.
(20) Flynn, J. H.; Wall, L. A. A Quick Direct Method for the Determination of Activation Energy from Thermogravimetric Data. *Polym. Lett.* **1966**, *4*, 232.
(21) Coats, A. W.; Redfern, J. P. Kinetic Parameters from Thermogravimetric Data. *Nature* **1964**, *20*, 68.
(22) Van Krevelens, D. W.; Hoftijzer, P. J. Kinetics of Gas−Liquid Reaction-General Theory. *Trans. I Chem. E* **1954**, *32*, 5360.
(23) Criado, J. M.; Pérez-Maqueda, L. A.; Sánchez-Jiménez, P. E. Dependence of the Preexponential Factor on Temperature. *J. Therm. Anal. Calorim.* **2005**, *82*, 671.
(24) Wang, Z.; Wang, J.; Dang, L. Thermal, Phase Transition and Spectral Studies in Erythromycin Pseudopolymorphs: Dihydrate and Acetone Solvate. *Cryst. Res. Technol.* **2006**, *41*, 1219.
(25) Zhang, K.; Hong, J.; Cao, G.; Zhan, D.; Tao, Y.; Cong, C. The Kinetics of Thermal Dehydration of Copper(II) Acetate Monohydrate in Air. *Thermochim. Acta* **2005**, *437*, 145.
(26) Takei, T.; Kameshima, Y.; Yasumori, A.; Okada, K. Crystallization Kinetics of Mullite From $Al_2O_3-SiO_2$ Glasses Under Non-isothermal Conditions. *J. Eur. Ceram. Soc.* **2001**, *21*, 2487.
(27) Ray, C. S.; Yang, Q.; Huang, W.-H.; Day, D. E. Surface and Internal Crystallization in Glasses as Determined by Differential Thermal Analysis. *J. Am. Ceram. Soc.* **1996**, *49*, 3155.
(28) Graetz, J.; Reilly, J. J. Decomposition Kinetics of the AlH_3 Polymorphs. *J. Phys. Chem. B* **2005**, *109*, 22181.
(29) Zhang, C.-T.; Wang, J.-K.; Wang, Y.-L. Non-isothermal Dehydration Kinetics of Ceftriaxone Disodium Hemiheptahydrate. *Ind. Eng. Chem. Res.* **2005**, *44*, 7057.
(30) Young, D. *Decomposition of Solids*; Academia: Prague, 1984.
(31) Rooney, J. J. Erying Transition-State Theory and Kinetics in Catalysis. *J. Mol. Catal. A: Chem.* **1995**, *96*, L1.
(32) Boonchom, B. Kinetics and Thermodynamic Properties of the Thermal Decomposition of Manganese Dihydrogenphosphate Dihydrate. *J. Chem. Eng. Data* **2008**, *53*, 1533–1538.
(33) Cordes, H. M. Preexponential Factors for Solid-State Thermal Decomposition. *J. Phys. Chem.* **1968**, *72*, 2185.

Received for review September 8, 2008. Accepted January 8, 2009. The financial support from the Development and Promotion in Science and Technology Talents Project (DPST) and the Center of Excellence for Innovation in Chemistry (PERCH-CIC) is acknowledged.

JE8006748